

ADVERTISEMENT



XV Collection:
**What Happens when the Antibiotic
1-2 Punch Backfires?**
Michael Laub discusses his favorite article in the journal

[plos.org](#)

[create account](#)

[sign in](#)



[Publish](#)

[About](#)

OPEN ACCESS PEER-REVIEWED

RESEARCH ARTICLE

N-Acetylcholinesterase-Induced Apoptosis in Alzheimer Disease

Debra Toiber, Amit Berson, David Greenberg, Naomi Melamed-Book, Sophia Diamant, Hermona Sor...

Published: September 1, 2008 • <https://doi.org/10.1371/journal.pone.0003108>

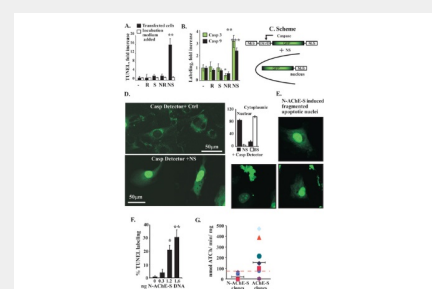
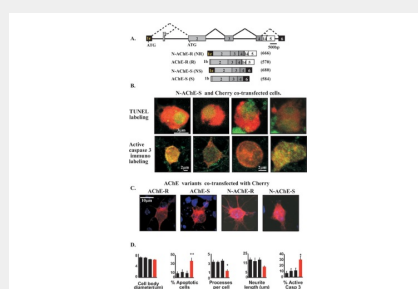
[Article](#) [Authors](#) [Metrics](#) [Comments](#)

Reader Comments (0)

Media Coverage

Figures

Figures



Abstract

Background

Alzheimer's disease (AD) involves loss of cholinergic neurons and Tau hyperphosphorylation. Here, we report that overexpression of an N-terminal "synaptic" acetylcholinesterase variant, N-AChE-S is causally involved in AD-related phenomena.

Methodology and Principal Findings

In transfected primary brain cultures, N-AChE-S induced cell death, Tau hyperphosphorylation and caspase 3 activation. Rapid internalization of fluorescently labeled fasciculin-2 to N-AChE-S transfected cells indicated membranous localization. In cortical cell lines, N-AChE-S transfection activated the Tau kinase GSK3, induced Tau hyperphosphorylation and caused apoptosis. N-AChE-S-induced cell death was reversed by inhibiting GSK3 or caspases, by enforced overexpression of the anti-apoptotic proteins, or by AChE inhibition or silencing. Moreover, inherent N-AChE-S-induced cell death was reversed by stressors inducing protein misfolding and calcium imbalances, but not by inhibitors of AD; and in cortical tissues from AD patients, N-AChE-S overexpression induced Tau hyperphosphorylation.

Conclusions

Together, these findings attribute an apoptogenic role to N-AChE-S and add new value to AChE inhibitor therapeutics in early AD.

Citation: Toiber D, Berson A, Greenberg D, Melamed-Book N, Dikler A, et al. (2008) N-Acetylcholinesterase-Induced Apoptosis in Alzheimer's Disease. *PLOS ONE* 3(9): e3108. <https://doi.org/10.1371/journal.pone.0003108>

Editor: Joseph Najbauer, City of Hope Medical Center, United States

Received: April 2, 2008; **Accepted:** August 8, 2008; **Published:** September 2, 2008

Copyright: © 2008 Toiber et al. This is an open-access article distributed under the terms of the Creative Commons Attribution License, which permits unrestricted use, distribution, and reproduction in any medium, provided the original author and source are credited.

Funding: This research was supported by the European Union's FP6 Excellence (LSH-2004-1.1.5-3) and STREP (LSHG-CT-2006-037277) programs, the Ministry of Science and German-Israeli Project, DIP-G 3.2, the Israel Science Foundation, the Interdisciplinary Center for Neuronal Computation (ICNC), and the ROSETREES Foundation, UK.

Introduction

In Alzheimer's disease (AD), premature death of cholinergic neurons, accumulation of neurofibrillary tangles, constituting of hyper-phosphorylated tau, and the cholinergic hypothesis attributes the cognitive impairments in AD to cholinergic dysfunction [1]. Accordingly, acetylcholinesterase (AChE) inhibitors seem to alleviate symptoms by prolonging acetylcholine (ACh) availability [2]. Some studies suggest that the disease process under treatment with AChE inhibitors [4, 5]; or alternative AD therapeutics, including inhibitors of the Tau kinase, Cdk5, and Kinase 3 (GSK3) [6, 7], or of other key proteins of the apoptotic pathway is unclear if these different approaches reflect a single targeted cascade that triggers this cascade.

Apoptotic cell death leads to cortical shrinkage in AD brains, accompanied by loss of cholinergic neurons, which express considerably more AChE than other cell types [8]. Recent reports demonstrated AChE accumulation in apoptotic cells, and inhibition and general silencing were found to prevent apoptotic cell death [9, 10]. Such cell death may occur through activation of the endoplasmic reticulum (ER), mitochondrial stress and/or cell surface death receptors [11], and recent reports raised a new question: how do AChE-expressing neurons survive? AChE is not one but several variants, induced by alternate promoters and alternative splicing [13]. It occurred to us that some, but not all, AChE variants, may be involved in neuronal cell death which occurs in AD. To challenge this theory, we overexpressed AChE variants in the AD cortex, tested the effects of aberrant AChE gene expression in cultured cells, explored the molecular mechanism(s) involved by measuring cell death and key apoptotic proteins, and searched for pharmacological mechanisms that might be mitigating the observed apoptotic effects.

Results

N-AChE-S expression induces caspase-mediated cell death

Overexpression of two short (AChE-S, AChE-R) and two N-terminally truncated (N-AChE-S, N-AChE-R) [13] (Fig 1A), was induced by transient transfection in primary cortical cells, HEK 293 embryonic kidney cells, U87MG glioblastoma cells, epithel and CHO hamster ovary cells. In primary cortical cells expressing N-AChE-S, apoptosis was invariably caused, observed as increased TUNEL labeling and caspase activation (Fig 1B and C, respectively). Surviving cortical cells transfected with N-AChE-S showed similar cell body size to those expressing the other variant, but they extended fewer and shorter processes from the cell body than cells transfected with other variants, indicating ill health for transfected surviving cells (Fig 1D). No other tested AChE variant exerted such effects (Fig 1E and Table S1). To rule out the possibility of indirect effects of secreted AChE or other proteins, by

pre-conditioned medium, removed 24 hr after transfection and add cells, caused no apoptotic effect (Fig 2A and Table S1). Together, th caused cell death to intracellular overexpression of N-AChE-S. More overexpressing cells showed concurrent increases in both activate 2B) and the caspase inhibitor Z-VAD-FMK prevented the N-AChE-S in below), suggesting a caspase-mediated apoptotic cascade [14]. Hi specificity of the N-AChE-S-induced effects, caspase 3 levels were i AChE-R-transfected cells (Fig 2B).Therefore, the N-terminal extensio be insufficient to cause the cell death conferred by N-AChE-S.



Download:

PPT [Pow](#)

PNG [larg](#)

TIFF [orig](#)

Figure 1. N-AChE-S induced apoptosis in primary cortical cells.

A. AChE mRNA transcripts. Upper scheme: The AChE gene structure codons are indicated. Lower scheme: corresponding transcripts open reading frames noted (amino acids). B. Primary cortical cell micrographs: N-AChE-S and Cherry cells co-transfected with (rec labeled (green). Lower micrographs: Red labeling as above, gre active caspase-3. C. Effects of AChE variants. Primary cortical cell transfection with Cherry and different AChE variants co-transfec show non apoptotic cells with different characteristics. N-AChE-S confers shrunk features. D. Shown are cell body diameters, perc cortical cells, No. of ramifications extended from cell bodies, ave length, and percent of cells labeled with caspase 3 activated an transfected with (from left to right) AChE-R, AChE-S, N-AChE-R and columns). Note N-AChE-S induced changes(*p=0.001,**p=0.000 <https://doi.org/10.1371/journal.pone.0003108.g001>



Download:

PPT [Pow](#)

PNG [larg](#)

TIFF [orig](#)

Figure 2. N-AChE-S induces caspase-mediated cell death.

A. N-AChE-S mediated apoptosis. TUNEL analysis 24 hr post-trans cells transfected with AChE variants or an "empty" plasmid, comp transfected cells incubated with pre-conditioned medium (*p=0.

test). B. Caspase immunostaining. N-AChE-S-associated increase in caspase 3 and 9 and N-AChE-R-associated reduction in caspase 3 and 9 (*p=0.04, **p=0.004, ***p=0.0003 Student's t test). C. Caspase-3 reporter. N-AChE-S was co-injected with GFP-NLS vector equipped with NEB caspase-cleavable DEVD motif. Caspase activation yields nuclear GFP translocation. D. Microinjection-induced caspase-mediated cell death. 3T3 cells co-injected with an "empty" plasmid and GFP-NES/NLS (left) showed cytoplasmic GFP, whereas N-AChE-S co-injected cells (right) showed nuclear fluorescence (columns). Shown are representative images. E. Within 24 hr from injection, cells exposed to N-AChE-S acquired nuclei with condensed chromatin. F. N-AChE-S-inducible apoptosis is dose-dependent. Percent of apoptotic U87MG cells under transient transfection increasing plasmid doses. (*p=0.03, **p=0.002 Student's t test). G. Transfection of N-AChE-S on cell viability. CHO cells were co-transfected with N-AChE-S vectors, and the G-418 antibiotic resistance plasmid, and grown for 7 days in the presence of G-418. Individual surviving clones were expanded and cellular AChE activity was measured (p=0.02, Student's t test) that individual clones transfected with N-AChE-S all showed considerably lower activity, largely below the average activity in human brain extract (<https://doi.org/10.1371/journal.pone.0003108.g002>).

To directly estimate the efficiency and dynamics of the N-AChE-S-induced apoptosis, we selected 3T3 cells for microinjecting N-AChE-S. Co-injection of a caspase-3 activated GFP reporter, equipped with a nuclear localization signal, allowed nuclear translocation to the nucleus in the presence of activated caspases and served for follow-up of the induced changes. The caspase reporter and GFP-NLS were microinjected for control (Fig 2D,E). Within 24 hrs, injection of GFP-NLS alone induced cytoplasmic GFP fluorescence in 94±3% of the cells (Fig 2D), whereas 85±3% of the N-AChE-S injected cells showed nuclear GFP fluorescence (Fig 2E). Caspase activation, and acquired condensed nuclei characteristic of apoptosis were observed in 70±3% of the cells (Fig 2E).

In cells transiently transfected with >1.2 ng/cell of the N-AChE-S DNA, we observed a dose-dependent apoptosis (Fig 2F). Next, individual clones of CHO cells that do not express any endogenous AChE variant were stably transfected with either full-length or shorter AChE-S, for comparison. Cloned cells presented considerably lower AChE activity than clones stably transfected with AChE-S (also called "tailor-made" AChE-S) reflected in considerably lower ACh hydrolytic activity than that of control cells transfected with AChE-S (10±8.4 vs. 150±45 nmol substrate hydrolyzed/min/mg protein) (Fig 2G, [dashed line](#)). Such low activities, lower than the average activity observed in human brain, indicated a possible selective pressure against expression of excess N-AChE-S levels. Thus, microinjection as well as transient and stable transfection of excess N-AChE-S is incompatible with cell viability.

N-AChE-S displays similar catalytic characteristics to other AChE variants

Fractionation and activity tests demonstrated that AChE-S and N-AChE-S were localized within the cells, whereas AChE-R and N-AChE-R both showed a tendency to be localized in the cytoplasm.

(Fig S1A). Sequence analysis predicted that while the AChE signal peptide is cleaved by the N-extended terminus, the new N-AChE variants include an acetylthioesterase domain. Higher expression levels for the shorter variants were observed by Western blot analysis of transiently transfected cells. Enzymatic Activity (with acetylthiocholine iodide) and native gels showed matched differences in enzyme activity (Fig S1B). The activity was proportional to the expression and activity of the various AChE proteins. No significant differences in enzymatic characteristics (e.g. K_m , substrate inhibition) were observed for N-AChE-S and N-AChE-R as compared with the shorter variants (Fig S1C,D), indicating that the extended variants are correctly folded. Thus, N-AChE-S was found to be expressed at lower levels than the shorter variants, but despite this, it was the one that induced the apoptogenic effect.

N-ACHE-S promotes GSK3 activation and Tau hyper-phosphorylation

The relatively low levels of N-AChE-S could potentially be due to misfolding-induced ER stress-activated apoptosis. To test this possibility, we measured the ER stress markers GRP78 and Xbp. Both GRP78 levels and the ratio of spliced and unspliced variants of Xbp were similar to those of cells transfected with shorter variants or control cells (Fig S2A,B), suggesting that the observed apoptosis was not caused by the misfolded protein response or the ACh hydrolysis. Nevertheless, high levels of N-AChE-S could signal the cell to undergo apoptosis, inducing another kind of cellular stress, compatible with other cases where overexpressed protein can lead to cell death, e.g. hIAPP in B cells [16]. The relevance to the observed apoptosis of the Tau kinase GSK3, which is involved in modulating Bcl proteins including Bax [17], [18] and was implicated in Alzheimer's pathology [19]. We tested the potential involvement of GSK3 in N-AChE-S-induced apoptosis in U87MG cells, which are more readily amenable for transfection than neurons. Supporting such involvement, N-AChE-S expression selected for cells with levels of inactive GSK3 carrying phosphorylated serine, whereas total GSK3 levels and levels of hyper-activated GSK3 with phosphorylated tyrosine were unchanged (Fig 3A). Thus, larger GSK3 fractions were active under N-AChE-S overexpression. Moreover, N-ACHE-S overexpression induced progressive increase in the phosphorylation of Tau in cultured U87MG cells, reaching a 37% increase after 48h transfection ($P < 0.05$, Fig 3B). Correspondingly, U87MG cells transfected with N-AChE-S showed 25% enhanced immunolabeling of activated Bax (Fig 3C), which was reduced by the GSK3 inhibitor SB316763, known to suppress cell death [18]. SB316763 reduced the immunolabeling of both activated Bax and hyper-phosphorylated Tau in cultured cells by about 20% as compared to N-AChE-S transfected cells (Fig 3D and data not shown). Also, SB316763 largely prevented the apoptogenic effect, to a similar extent as caspase inhibition, and without affecting cell viability (Fig 3D,E).



Download:

PPT PowerPoint

Figure 3. N-AChE-S induces suppressible GSK3-activation, Tau hyper-phosphorylation and Bax activation.

A. Immunoblots. N-AChE-S reduces serine-phosphorylated P-GSK3 β maintaining unchanged total GSK3 β and tyrosine phosphorylation, elevating active-Bax. B. Tau hyper-phosphorylation: N-AChE-S, but not N-AChE-R induces progressive increases in hyper-phosphorylated Tau. Alpha tubulin 4 served as reference. C. N-AChE-S-inducible GSK3 β dephosphorylation facilitates Bax activation. Shown are micrographs of transfected cells with elevated phosphorylated Bax labeling compared to control (Ctrl) cells. GSK3 inhibition suppresses this labeling. Quantification shows a significant increase in Bax labeling of NS overexpressing cells, preventable by SB316763 treatment (**p=0.00009 Student's t test). D. GSK3 inhibition suppress N-AChE-S-induced apoptosis. % TUNEL labeling of transfected cells. Note that 5 μ M SB316763 (GSK3-I) and 80 μ M Z-VAD-FMK (caspase-I) reduced apoptosis. (GSK-I p=0.000013, Casp3-I p=9.0e-05 Student's t test). E. GSK3 and Caspase inhibitors do not affect AChE catalytic activity. U87MG cells co-transfected with N-AChE-S and Bcl-2 (# p=0.00001), BI (*p=0.03), or Bcl-XL (p=0.054) showed variably suppressed TUNEL labeling.

<https://doi.org/10.1371/journal.pone.0003108.g003>

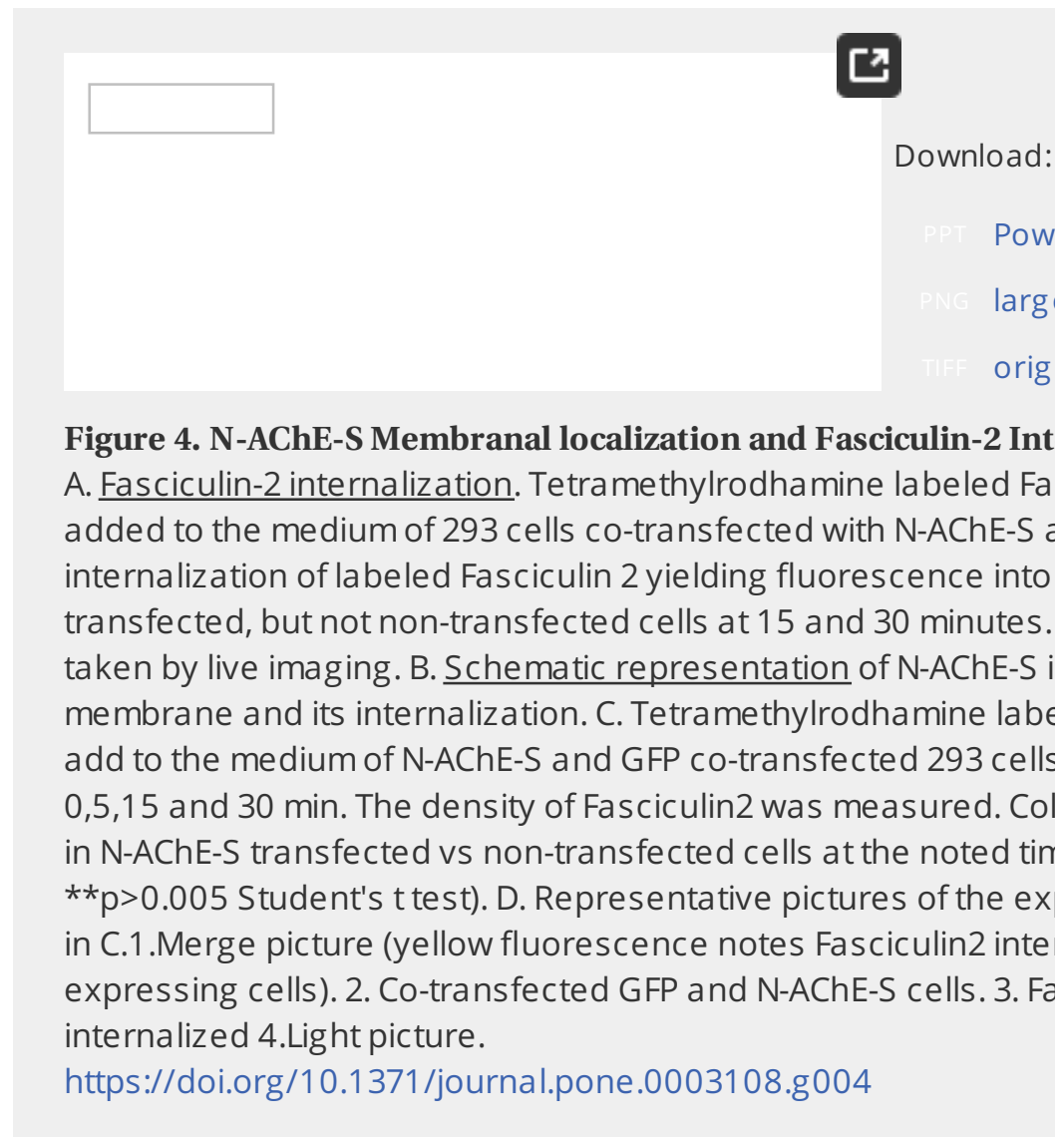
Bcl proteins mitigate the N-AChE-S induced apoptosis

Since AChE silencing was shown to prevent apoptosome formation, the N-AChE-S effect occurs upstream to the mitochondrial membrane permeabilization, a characteristic of apoptosis. Cultured cells were co-transfected with an apoptotic protein Bcl-2 or its family members, Bcl-xL and BI. All of the Bcl proteins prevented Bax from triggering the permeabilization of mitochondrial membrane and thus the N-AChE-S-induced cell death (Fig 3F), compatible with the notion that Bcl proteins act in the early apoptotic pathway.

Cell surface N-AChE-S location

We considered the possibility that in the N-extended AChE variants, the signal peptide can be used as transmembranal domain similar to that of the neuroligin [20]. To address this issue, we labeled Fasciculin-2, an AChE impermeable to the cell membrane, with tetramethyl-rhodamine (Fas2*) which do not express endogenous AChE were co-transfected with GFP. Cells were imaged 18 hrs and were exposed to Fas2*. Live imaging was performed before and every 5 minutes after its addition. Cells co-transfected with GFP and Fas2* transfected neighbor cells showed vesicular internalization of Fas2* as indicated by the red labeling. Cells transfected with GFP and Fas2* performed the same experiment and fixed cells after 0, 5, 15 or 30 minutes. The red labeling was disrupted the vesicles; however, red labeling reflecting internalized Fas2* was observed in the cytoplasm of cells expressing GFP+N-AChE-S compared to control c

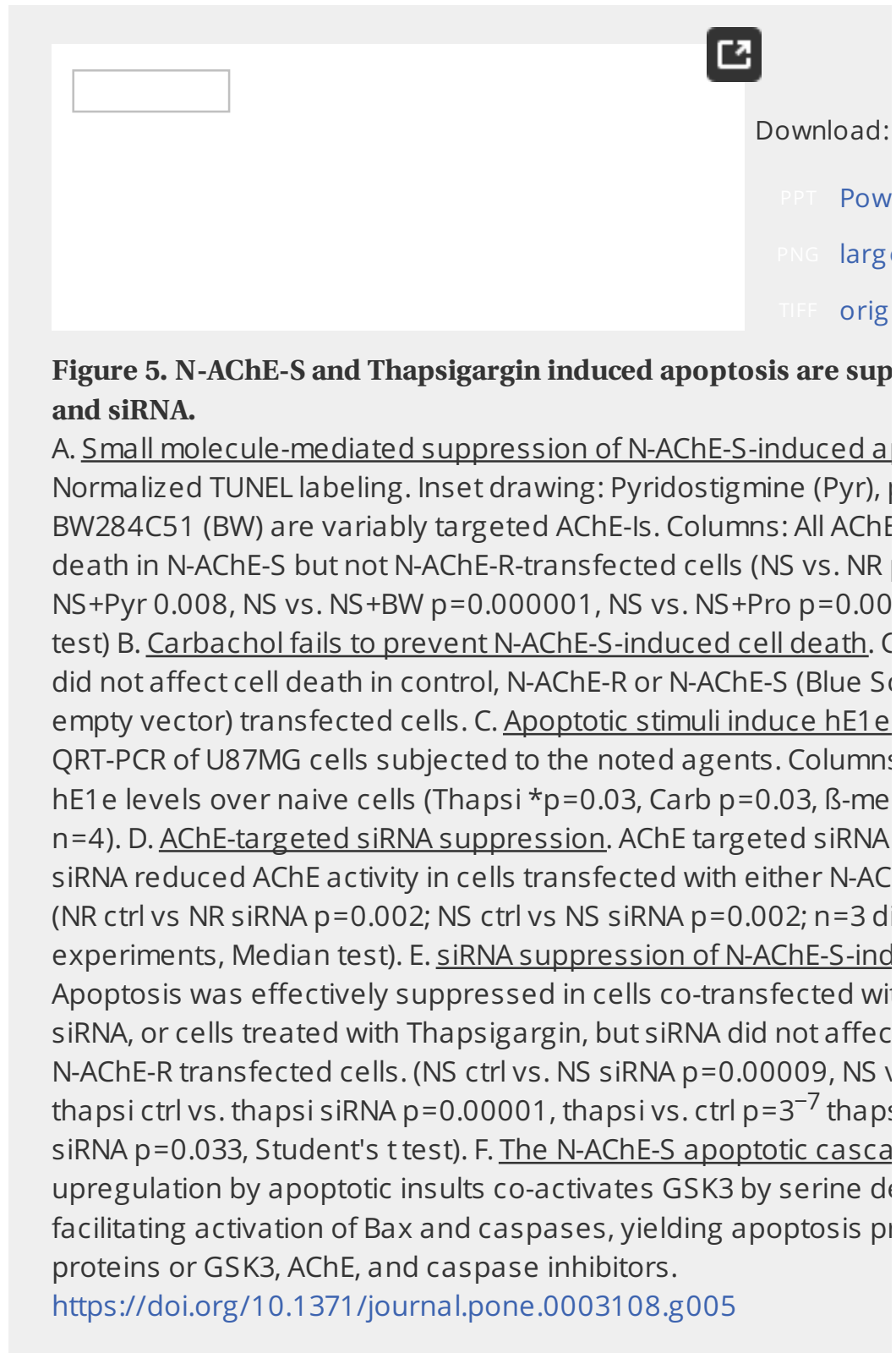
peaked after 5 minutes from Fas2* addition, remained unchanged and declined after 30 minutes. Our results indicate that N-AChE-S is positioned in the membrane with the catalytic domain towards the extracellular space and the extended N-terminal domain towards the intracellular space. In addition, we used antibodies specific for the extended N-terminal domain in comparison to antibodies targeted to the core domain to label N-AChE-S in U87MG cells. An “empty” vector served as control (Fig S3A, scheme). In electron microscopy, N-AChE-S-transfected cells yielded generally similar localization patterns with the N-specific and core domain antibodies, peaking at the cellular membrane (Fig S3A,B). Apart from the membrane-associated localization, 11% of the gold beads adhered to endocytotic vesicles (identified by their circular contours [23], compatible with the Fas2* data.



Core domain contributions to N-AChE-S-induced apoptosis

At the extracellular domain of synaptic membranes, neurexin interactions transduce intracellular signals through synaptic protein partners [24]. In addition, and electron microscopy results, we speculated that the intracellular domain of N-AChE-S might similarly mediate intracellular signaling in response to ligand binding. Given that inhibitor interactions induce structural changes in the AChE active site, we assessed the capacity of the carbamate active site inhibitor, pyridostigmine, a peripheral site inhibitor of AChE, propidium or the quaternary AChE inhibitor, physostigmine, known to be impermeable to the cell membrane [25] to affect N-AChE-S

apoptosis. All of these agents reduced apoptosis in N-AChE-S-transfected cells. The levels observed in N-AChE-R transfected or control cells (Fig 5A). This demonstrated inherent involvement of the core domain of AChE, which is embedded, in the N-AChE-S-induced apoptotic process. The simple mechanism(s) involved therefore suggests that the N-AChE-S-induced apoptosis initiates extracellularly, as it is susceptible for suppression by small molecules excluded from cellular entrance (e.g. BW284C51) and since such inhibitors prevent the transduction of the signal into the cell.



Since N-AChE-S is enzymatically active, we further wished to test whether cells were dying because of the lack of ACh. Addition of the non-degradable carbachol did not change the observed cell death (Fig 5B), excluding enzymatic involvement, suggesting structural, rather than enzymatic involvement of the core domain.

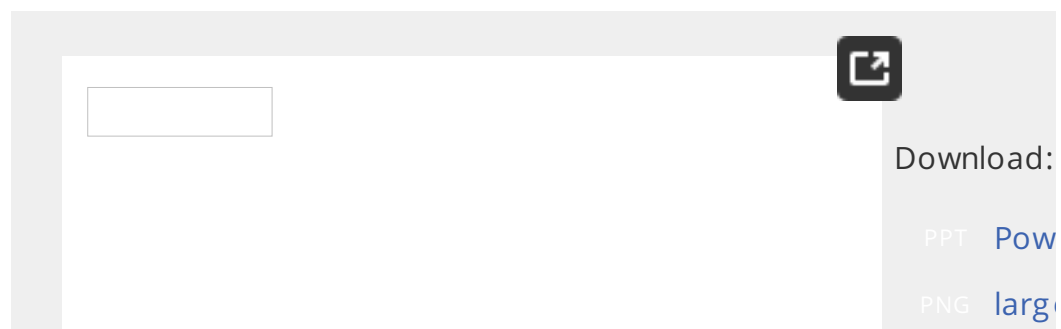
induced cell death.

Insult stimuli facilitate inherent N-AChE-S expression a

Notably, various cellular and organismal stimuli induce AChE overexpression, alternative splicing and alternate promoter choices [13], [26], [27]. Therefore, various stressors-induced gain of N-AChE-S function on apoptosis outcome. Treatment with mercaptoethanol, a reducing agent which denatures proteins by breaking disulfide bonds (0.2 M), or thapsigargin, which releases calcium from the ER (10 μ M) [28] all induced significant inherent overexpression of the full-length N-AChE-S with the extended N-terminus in U87MG cells (median test $p < 0.03$). In contrast, treatment with NMDA receptor agonist (0.5 mM), and cortisol, a glucocorticoid hormone, in U87MG cells from acute stress responses (0.5 μ M) [29] showed no effect on N-AChE-S expression (Fig 5C). This called for testing the consequences of loss of N-AChE-S function in U87MG cells co-transfected with N-AChE-S and an AChE-targeted siRNA, loss of N-AChE-S expression selectively abolished its apoptotic effect. siRNA also abolished cell death induced by thapsigargin; in comparison, suppressed N-AChE-S expression by cortisol treatment had no effect (Fig 5D,E). Thus, inherent gain of N-AChE-S function induced apoptosis, whereas loss of its function suppressed it. Together, these results identified N-AChE-S as an upstream apoptotic trigger encompassing "classical" cell death elements (Fig 5F) and likely acting through the unknown intracellular element(s) with the N-terminal extended domain.

N-AChE-S expression in AD

Last, but not least, we turned to the AD brain. When protein from cortex was differentially extracted in detergent and salt-containing solutions, AChE activity showed reduced AChE activity as compared to matched non-demented cortex. Reduction was observed in the membrane-associated fraction (which contains AChE-S) [30] (Fig 6A). Neither the soluble nor the membrane protein fraction decreases, indicating that the reduction was primarily of AChE-S, likely due to loss of cholinergic neurons. In NDC cortices, quantitative real-time PCR of each cDNA clone showed that transcripts spanning the hE1 exon and the N-terminal extension represent approximately 6% of total AChE mRNA (1,700 transcripts per ng RNA, compared to 55,700 transcripts of total AChE mRNA per ng RNA). In AD cortex, that both the core domain and the major exon 6 decreased by 40% or more compared with NDC cortical tissues (Fig 6B, and data not shown). Thus, AD cortex contained less AChE-S (which normally constitutes 90% of the enzymic activity) in amounts as NDC of N-AChE and AChE-R (each constituting about 6% of total transcripts).



A download options menu is visible in the bottom right corner of the page. It features a dark square icon with a white arrow pointing outwards. Below the icon, the text "Download:" is followed by two options: "PPT" and "PowerPoint", and "PNG" and "large image".

Figure 6. N-AChE-S overexpression in AD cortical neurons associated with hyper-phosphorylation.

A. Differential fractionation of AChE hydrolytic activity. Cortical protein was fractionated into low salt (LS, soluble protein), low salt detergent (LSD, associated) and high salt (HS, integral membrane and nuclear protein) fractions. AChE activity was measured. Note decrease in LSD (AChE-S-enriched) or HS fractions ($p=0.0476$, $n=4$ NDC, 8AD, Median test). B. AD-associated AChE mRNA transcripts. Columns: QRT-PCR. Note AD-associated increase in AChE-S mRNA compared to NDC samples in the S, but not the N or R encoding exons 10 AD, 5 NDC Wilcoxon Two Sample Test). C. Inset is: E1e labeling of AChE-S in AD and NDC cortices. Columns are quantification of AChE-S labeling density per area. (Median test, $*p=0.0286$, $n=4$ in each group). D. Immunostaining in AD and NDC cortices. Columns are quantification of AChE-S labeling density per area ($*p=0.029$ $n=5$ NDC, 9AD Median Test). E. AD Entorhinal cortex immunolabeled for N-AChE, AChE-S or hyper-phosphorylated Tau. Columns are quantification of AChE-S labeling density per area. (Median test, $*p=0.0286$, $n=4$ in each group). F. AChE-S labeling correlate with Tau-P density. Tau-P, N-AChE, and AChE-S were quantified using immunohistochemistry on sections from the entorhinal cortex of AD patients. (Pearson's correlation for N-AChE and Tau-P, $r=0.78$, $n=10$, $p<0.001$ <https://doi.org/10.1371/journal.pone.0003108.g006>)

Our mRNA analyses suggested that in the remaining cholinergic neurons, N-AChE-S constitutes a larger part of AChE than in NDC brains. To challenge this hypothesis, we used quantified FISH analysis which indeed identified 273% enhanced AChE-S labeling in AD cortical cells with neuronal morphology as compared with NDC samples ($p=0.03$) (Fig 6C). Immuno-labeling further demonstrated 152% elevated AChE-S labeling in AD compared to NDC cortices (Fig 6D), together suggesting AD-associated overexpression of N-AChE-S in AD neurons.

Association with hyper-phosphorylated Tau in AD

Tau hyper-phosphorylation is a marker of AD pathology that is directly linked to neuronal death. Importantly, N-AChE and AChE-S showed similar patterns of expression as hyper-phosphorylated Tau in the AD cortices. The majority (72, 70%) of cells out of approximately 100 in each group) of cells expressing N-AChE-S and hyper-phosphorylated Tau were 7–24 μm in length, compatible with the size of pyramidal neurons (Fig 6E). Moreover, the labeling intensity of N-AChE, and to a somewhat lesser extent AChE-S (probably because only part of the AChE-S molecules are N-AChE-S) were correlated with that of hyper-phosphorylated Tau (Fig 6F). Together these observations are compatible with the hypothesis that N-AChE-S overexpression in AD cortical neurons is causally linked with the apoptotic destiny of neurons expressing hyper-phosphorylated Tau.

Discussion

Recent reports of AChE association with apoptosis [9], [10] left unclear the survival of AChE-expressing cholinergic neurons. Our current findings provide an unequivocal answer to this question by pointing at N-AChE-S as the variant. We further demonstrate that N-AChE-S induces cell death only above a critical threshold. To explore the molecular mechanism(s) of its apoptotic role, and to study its relevance for the AD-induced death, we systematically manipulated N-AChE-S expression in cell culture and demonstrated that gain of N-AChE-S function invariably induces apoptosis, while its function improves survival.

Enforced N-AChE-S overexpression induced apoptosis both in primary and in different cell lines of various tissue and organismal origins. This attests to a conserved and ubiquitous role as a general trigger of apoptosis. In AD, neuronal loss reaches 30–90% [31] in a manner attributable to the hyperphosphorylated Tau and neurofibrillary tangles [1]. Circulation AChE is elevated during normal aging [32]; moreover, the ApoE4 genotype [33], mutations in APOE4 and the presence of A β [35]–[37] all induced upregulation of AChE and this upregulation was also reported as being induced by the apoptotic process, as well as by damaging light in retinal neurons [39]. Here we report that the reactions and calcium misregulation, both implicated in AD and in neuronal death [40], lead to N-AChE-S overexpression. Our current findings that the protein involved in all the above phenomena was likely the N-AChE-S variant. Further studies will be required to explore the possible function(s) of N-AChE-S and define if it is involved, for example in the programmed cell death of developing neurons [41].

The N-AChE-S, but not the N-AChE-R or the shorter AChE-S variants is involved, suggesting that both the N- and the-S termini are required for this process. Various AChE inhibitors suppressed the N-AChE-S induced apoptosis, suggesting a central core domain, where AChE's active site is embedded [42] as well as the N-terminus is involved as well. The most likely explanation for this multi-domain involvement is structural, rather than enzymatic features of N-AChE-S protein are involved. The N-terminus of N-AChE-S variant to the cell membrane and demonstrate interactions and rapid internalization for this protein, suggesting that the N-terminus of N-AChE-S protrudes intracellularly, similar to the homologue of neuroligin [20]. Inhibitor interactions were shown by others to exert effects on the AChE molecule [43], indicating parallel changes in N-AChE-S. The fact that inhibitors attenuate the N-AChE-S-induced apoptotic outcome there suggests that the core domain transduces signals to the cell through the cytoplasmic tail. Together, this implies that N-AChE-S likely operates as a bifunctional protein with properties characteristic of both enzymes and ligand-activated receptors. In light of the above arguments, these findings may also explain the reported effects of anticholinesterases [4], [5] and can possibly outline testis-protective prophylactic agents.

Our current finding of increased N-AChE expression in AD cortices, together with their core AChE expression and activity, is compatible with the enhanced activity of these tissues. Supporting the notion of causal relationship with this finding, stress and calcium imbalances have been implicated in GSK3 activation

in the AD brain [12] through hyper-phosphorylated Tau, presenilin, and N-ACHE-S-induced dephosphorylation of the Ser residue activating properties corroborates this association. Others reported increase staining in neurons with Tau hyper-phosphorylation. A recent report that Tau hyper-phosphorylation is protective [44]. Our findings did not resolve between these possibilities but demonstrate apparent association of hyper-phosphorylation with the N-AChE-S apoptotic mechanism. We further demonstrate that exposure to apoptotic stressors would likely induce N-AChE-S expression in the cholinergic neurons with higher basal AChE expression, and cause neuronal death. At least part of the currently employed AD therapeutics may be aimed at reducing this overexpression by preventing the N-AChE-S-induced apoptotic mechanism of disease progression [4], [5]. Further delineation of this induction and its role for preventing the premature death of cholinergic neurons at earlier stages of disease would therefore merit special attention.

Materials and Methods

Human brain tissue

Brain tissue from AD patients (n=10) and matched non-demented controls was obtained from The Netherlands Brain Bank. Ethical approval and written informed consent from the donors or the next of kin was obtained in all cases. Neurofibrillary staging of neurofibrillary changes (I–VI) was performed *post mortem*.

Primary cortical cell culture

Cerebral cortex was separated from the brain of 15th day embryos and cells plated on poly-L-ornithine coated cover slips in Neurobasal medium supplemented with Glutamax and Penicillin/streptomycin (Invitrogen). Transfection was performed with lipofectamine 2000 (Invitrogen).

Plasmids

The N-AChE-R and N-AChE-S plasmids are modifications of CMV-AChE-R with the hE1 exon inserted in the HindIII cloning sites. Bax Inhibitor-1 was from Santa Cruz Biotechnology (Santa Cruz, CA), and the caspase detector was from BD Biosciences (San Jose, CA).

Microinjection

NIH 3T3 cells were microinjected using an Axiovert200M Zeiss microscope with a microinjection system, incubated for 24 hours and then viewed. The microscope was equipped with a 1024 BioRad confocal scanhead coupled to a Zeiss Axiovert 135M microscope with a 40×/NA=1.3 oil immersion objective. GFP was detected at 488 nm excitation wavelength and a HQ525±20 filter served for collecting emission.

Statistics Methods

Student's t-test was used in cell culture experiments, where cell number was high enough to assume normal distribution.

Median test is a non-parametric test was used for comparing the media of two populations that were relatively small, assuming abnormal distribution. It was used for samples, maximum 10 e.g. mRNA transcripts, protein densities and compared to control.

The Wilcoxon test was preferred over the median test when one or more samples were "off scale". It served for calibrating cDNA transcripts from AD and control.

Pearson correlation test describing the strength of an association between two variables. It was used to measure the correlation between N-AChE-S and hyper-phosphorylation. The aim was to test if *linear* relationship exists between these values of phosphorylation and N-AChE-S.

Image analysis

Immunohistochemistry and In situ hybridization experiments were analyzed using ImageJ 1.33 free software (<http://rsb.info.nih.gov/ij/>).

1. In the "Analyze tool" we chose Set measurements and selected: Mean gray value (which measures the density of the selected pixels divided by the number of pixels) to quantify staining intensity.

2. We used the "freehand selection" tool to draw a line around a single cell to measure and then selected an appropriate measure in the "analyze" menu. We analyzed many cells (20–30) in each picture. We selected 2–3 empty cells to determine the background for each picture, and subtracted it from the observed for the measured cells to normalize light efficiency differences between different pictures.

3. The total average for a single experiment was composed of 4 different pictures. Standard deviation values were calculated for these averages, to check the possibility that a specific change was an outlier which occurred out of the range calculated for the other pictures.

The averages of the different groups were used and are depicted in the results section.

4. Data collected from the different cells in each picture was used to calculate the mean value for that picture. In case of cell culture experiments, 5–8 different pictures were used to assess each treatment and were analyzed as noted before.

5. For Western Blot analysis we used the ImageJ Gel Analyzer option to draw a rectangular shape for each band in the gel. We captured the gray value of the band, which should correlate with the quantity of protein. We used the areas measured as reflecting protein quantity. Normalization was done by dividing the area by that obtained for tubulin 4 from that sample, which serves as a housekeeping standard.

Supplementary methods

Immunohistochemistry, confocal and electron microscopy, fluorescence hybridization (FISH), cell cultures, siRNA design and production and were as described [45] (and/or are all detailed under Supplementa

Real Time PCR, TUNEL Apoptosis assay, immunocytochemistry, prote described [46] (Text S1, Table S3 antibodies list and Table S4 probe

Supporting Information

Text S1.

Supplementary Materials and Methods.

<https://doi.org/10.1371/journal.pone.0003108.s001>

(0.05 MB DOC)

Figure S1.

N-AChE-S characteristics. A. Cellular and secreted AChE forms. Hydrolytic activity of AChE variants in transiently transfected U87MG cell extracts and media. AChE-R and N-AChE-R are largely secreted, whereas AChE-S and N-AChE-S are mostly cellular. Immunoblot and activity staining. Top: Immunoblot. Note low-level expression of AChE-S and N-AChE-R compared to the corresponding shorter counterparts. Bottom: Activity staining in a native gel. Note migration and staining intensity differences. Percentage of maximal acetylthiocholine (ATCh) hydrolytic activity as a function of substrate concentration. Note indistinguishable K_m values (0.33 ± 0.04 , 0.35 ± 0.13 , and 0.39 ± 0.17) and similar Hill's coefficients (0.94 ± 0.12 , 0.87 ± 0.18) for the AChE-R, AChE-S, N-AChE-R and N-AChE-S variants, respectively. Substrate inhibition. All variants showed inhibition under acetylthiocholine concentrations >5 mM.

<https://doi.org/10.1371/journal.pone.0003108.s002>

(1.42 MB TIF)

Figure S2.

N-AChE-S Sustained Unfolded protein Response under Transfection. Immunoblot shows similar levels of GRP78, an unfolded protein response marker, in cells co-transfected with AChE-S, N-AChE-R and N-AChE-S. B. XBP splicing analysis shows the PCR products of XBP transcripts, the upper band is the unspliced form and the lower band is the spliced form. N-AChE-S transfection sustained a similar ratio of unspliced/spliced forms to those seen with the other AChE variants. ER stress (below) showed higher expression of XBP and a higher ratio of unspliced/spliced forms (columns).

<https://doi.org/10.1371/journal.pone.0003108.s003>

(1.30 MB TIF)

Figure S3.

Membranal localization of N-AChE-S. Top Scheme: Antibodies to the domain of N-AChE-S (NS). SP: Original signal peptide. A. Electron mic decorated antibodies labeling of U87MG cells transfected with N-AChE-S close to the plasma membrane or within endocytotic, clathrin-coated vesicles. Labeling distribution. Columns: Distance of gold beads from the plasma membrane. Intracellular N-AChE-S labeling for both the N-terminus and the core domain. 11% - in endocytotic vesicles.

<https://doi.org/10.1371/journal.pone.0003108.s004>

(1.86 MB TIF)

Table S1.

<https://doi.org/10.1371/journal.pone.0003108.s005>

(0.07 MB DOC)

Table S2.

<https://doi.org/10.1371/journal.pone.0003108.s006>

(0.04 MB DOC)

Table S3.

<https://doi.org/10.1371/journal.pone.0003108.s007>

(0.04 MB DOC)

Table S4.

<https://doi.org/10.1371/journal.pone.0003108.s008>

(0.03 MB DOC)

Acknowledgments

We thank Dr Gabriel Nunez (Michigan) for the Bcl-2 and Bcl-XL plasmids.

Author Contributions

Conceived and designed the experiments: DT HS. Performed the experiments: DT HS. Analyzed the data: DT NMB HS. Contributed reagents/materials/analysis tools: DT HS. Wrote the paper: DT HS.

References

1. Arriagada PV, Growdon JH, Hedley-Whyte ET, Hyman BT (1999)

tangles but not senile plaques parallel duration and severity of disease. *Neurology* 42: 631–639.

[View Article](#) • [Google Scholar](#)

2. Whitehouse PJ, Price DL, Struble RG, Clark AW, Coyle JT, et al. (1981) Neurofibrillary tangles and senile dementia: loss of neurons in the basal forebrain. *Ann Neurol* 10: 1237–1239.

[View Article](#) • [Google Scholar](#)

3. Mesulam M (2004) The cholinergic lesion of Alzheimer's disease: a side show? *Learn Mem* 11: 43–49.

[View Article](#) • [Google Scholar](#)

4. Nordberg A (2006) Mechanisms behind the neuroprotective effects of cholinesterase inhibitors in Alzheimer disease. *Alzheimer Dis* 18: S12–18.

[View Article](#) • [Google Scholar](#)

5. Recanatini M, Valenti P (2004) Acetylcholinesterase inhibitors: towards improved Alzheimer's disease therapeutics. *Curr Pharm Biotechnol* 5: 3166.

[View Article](#) • [Google Scholar](#)

6. Huang HC, Klein PS (2006) Multiple roles for glycogen synthase kinase-3 as a target in Alzheimer's disease. *Curr Drug Targets* 7: 1389–1399.

[View Article](#) • [Google Scholar](#)

7. Bhat RV, Budd Haeberlein SL, Avila J (2004) Glycogen synthase kinase-3 as a target for CNS therapies. *J Neurochem* 89: 1313–1317.

[View Article](#) • [Google Scholar](#)

8. Landwehrmeyer B, Probst A, Palacios JM, Mengod G (1993) Expression of acetylcholinesterase messenger RNA in human brain: an immunohistochemical study. *Neuroscience* 57: 615–634.

[View Article](#) • [Google Scholar](#)

9. Park SE, Kim ND, Yoo YH (2004) Acetylcholinesterase plays a role in apoptosis formation. *Cancer Res* 64: 2652–2655.

[View Article](#) • [Google Scholar](#)

10. Zhu H, Gao W, Jiang H, Jin QH, Shi YF, et al. (2007) Regulation of acetylcholinesterase expression by calcium signaling during A23187- and thapsigargin-induced apoptosis. *Int J Biochem*

- 11.** Dickson DW (2004) Apoptotic mechanisms in Alzheimer neurodegeneration: cause or effect? *J Clin Invest* 114: 23–27.
[View Article](#) • [Google Scholar](#)
- 12.** Mattson MP (2000) Apoptosis in neurodegenerative disorders. *Nat Rev Neurosci* 1: 120–129.
[View Article](#) • [Google Scholar](#)
- 13.** Meshorer E, Soreq H (2006) Virtues and woes of AChE alternative related neuropathologies. *Trends Neurosci* 29: 216–224.
[View Article](#) • [Google Scholar](#)
- 14.** Danial NN, Korsmeyer SJ (2004) Cell death: critical control point. *Nat Rev Mol Cell Biol* 5: 349–359.
[View Article](#) • [Google Scholar](#)
- 15.** Massoulie J (2002) The origin of the molecular diversity and function of cholinesterases. *Neurosignals* 11: 130–143.
[View Article](#) • [Google Scholar](#)
- 16.** Huang CJ, Haataja L, Gurlo T, Butler AE, Wu X, et al. (2007) Endoplasmic reticulum stress-induced beta-cell apoptosis and accumulation of polyubiquitinated proteins by human islet amyloid polypeptide. *Endocrinol Metab* 293: E1656–1662.
[View Article](#) • [Google Scholar](#)
- 17.** Linseman DA, Butts BD, Precht TA, Phelps RA, Le SS, et al. (2002) p38 kinase-3beta phosphorylates Bax and promotes its mitochondrial translocation during neuronal apoptosis. *J Neurosci* 24: 9993–10002.
[View Article](#) • [Google Scholar](#)
- 18.** Jope RS, Johnson GV (2004) The glamour and gloom of glycogen synthase kinase-3. *Trends Biochem Sci* 29: 95–102.
[View Article](#) • [Google Scholar](#)
- 19.** Russ C, Lovestone S, Powell JF (2001) Identification of sequential phosphorylation sites in glycogen synthase kinase-3beta and analysis of the role of the glycogen synthase kinase 3 beta in late onset Alzheimer's disease. *Mol Psychiatry* 6: 320–324.
[View Article](#) • [Google Scholar](#)
- 20.** Ichtchenko K, Nguyen T, Sudhof TC (1996) Structures, alternative splicing, and functions of syntaxin 1. *Neuron* 17: 105–116.
[View Article](#) • [Google Scholar](#)

neurexin binding of multiple neuroligins. *J Biol Chem* 271: 267-271.
[View Article](#) • [Google Scholar](#)

21. Peng HB, Xie H, Rossi SG, Rotundo RL (1999) Acetylcholinesterase at the neuromuscular junction involves perlecan and dystroglycan. *J Biol Chem* 274: 9185-9191.

[View Article](#) • [Google Scholar](#)

22. Meshorer E, Toiber D, Zurel D, Sahly I, Dori A, et al. (2004) Co-expression of 5' alternative acetylcholinesterase transcripts and proteoglycans in the neuromuscular junction. *J Biol Chem* 279: 29740-29751.

[View Article](#) • [Google Scholar](#)

23. Higgins MK, McMahon HT (2002) Snap-shots of clathrin-mediated endocytosis. *Trends Biochem Sci* 27: 257-263.

[View Article](#) • [Google Scholar](#)

24. Bourne Y, Kolb HC, Radic Z, Sharpless KB, Taylor P, et al. (2000) A small molecule inhibitor captures acetylcholinesterase in a unique conformation. *Proc Natl Acad Sci U S A* 101: 1449-1454.

[View Article](#) • [Google Scholar](#)

25. Mc IR, Koelle GB (1959) Comparison of the effects of inhibitory and total acetylcholinesterase upon ganglionic transmission. *J Biol Chem* 236: 9-20.

[View Article](#) • [Google Scholar](#)

26. Kaufer D, Friedman A, Seidman S, Soreq H (1998) Acute stress induces lasting changes in cholinergic gene expression. *Nature* 393: 81-85.

[View Article](#) • [Google Scholar](#)

27. Meshorer E, Erb C, Gazit R, Pavlovsky L, Kaufer D, et al. (2002) Neuritic mRNA translocation under long-term neuronal stress. *Science* 295: 508-512.

[View Article](#) • [Google Scholar](#)

28. Thastrup O, Cullen PJ, Drobak BK, Hanley MR, Dawson AP (1990) The tumor promoter, 12-O-tetradecanoylphorbol-13-acetate, discharges intracellular Ca²⁺ stores by specific activation of endoplasmic reticulum Ca²⁺-ATPase. *Proc Natl Acad Sci U S A* 87: 100-104.

[View Article](#) • [Google Scholar](#)

29. Kaufer D, Ogle WO, Pincus ZS, Clark KL, Nicholas AC, et al. (2000) The neuronal stress response with anti-glucocorticoid gene deletion. *J Biol Chem* 275: 10000-10006.

947–953.

[View Article](#) • [Google Scholar](#)

- 30.** Soreq H, Seidman S (2001) Acetylcholinesterase–new roles
Rev Neurosci 2: 294–302.

[View Article](#) • [Google Scholar](#)

- 31.** Killiany RJ, Gomez-Isla T, Moss M, Kikinis R, Sandor T, et al. (2000) Functional magnetic resonance imaging to predict who will get Alzheimer's disease
Neurol 47: 430–439.

[View Article](#) • [Google Scholar](#)

- 32.** Sklan EH, Lowenthal A, Korner M, Ritov Y, Landers DM, et al. (2002) The relationship between Acetylcholinesterase/paraoxonase genotype and expression levels and cognitive scores in Health, Risk Factors, Exercise Training, and Genetics Study
Acad Sci U S A 101: 5512–5517.

[View Article](#) • [Google Scholar](#)

- 33.** Eggers C, Herholz K, Kalbe E, Heiss WD (2006) Cortical acetylcholinesterase activity and ApoE4-genotype in Alzheimer disease. Neurosci Lett 400: 105–108.

[View Article](#) • [Google Scholar](#)

- 34.** Nguyen HN, Hwang DY, Kim YK, Yoon DY, Kim JH, et al. (2005) Curcumin increases acetylcholinesterase activity in neuronal cells. Arch Biochem Biophys 435: 1073–1078.

[View Article](#) • [Google Scholar](#)

- 35.** Carroll RT, Lust MR, Emmerling MR (1999) Beta-amyloid levels and acetylcholinesterase activity in human cerebrospinal fluid. Neurosci Lett 267: 105–108.

[View Article](#) • [Google Scholar](#)

- 36.** Hu W, Gray NW, Brimijoin S (2003) Amyloid-beta increases acetylcholinesterase expression in neuroblastoma cells by reducing enzyme degradation
J Neurosci 23: 470–478.

[View Article](#) • [Google Scholar](#)

- 37.** Sberna G, Saez-Valero J, Beyreuther K, Masters CL, Small DH (2002) The beta-protein of Alzheimer's disease increases acetylcholinesterase activity by increasing intracellular calcium in embryonal carcinoma P19 cells
Neurosci Lett 325: 1177–1184.

[View Article](#) • [Google Scholar](#)

- 38.** Deng R, Li W, Guan Z, Zhou JM, Wang Y, et al. (2006) Acetylcholinesterase activity and ApoE4 genotype in Alzheimer disease. Neurosci Lett 400: 105–108.

expression mediated by c-Jun-NH2-terminal kinase pathway drug-induced apoptosis. *Oncogene* 25: 7070–7077.

[View Article](#) • [Google Scholar](#)

- 39.** Kehat R, Zemel E, Cuenca N, Evron T, Toiber D, et al. (2007) A acetylcholinesterase exacerbates photoreceptors death of Ophthalmol Vis Sci 48: 1290–1297.

[View Article](#) • [Google Scholar](#)

- 40.** Toiber D, Soreq H (2005) Cellular stress reactions as putative Alzheimer's disease. *Neurochem Res* 30: 909–919.

[View Article](#) • [Google Scholar](#)

- 41.** de la Rosa EJ, de Pablo F (2000) Cell death in early neural development: neurotrophic theory. *Trends Neurosci* 23: 454–458.

[View Article](#) • [Google Scholar](#)

- 42.** Sussman JL, Harel M, Frolow F, Oefner C, Goldman A, et al. (1997) Structure of acetylcholinesterase from *Torpedo californica*: a prototypic binding protein. *Science* 253: 872–879.

[View Article](#) • [Google Scholar](#)

- 43.** Millard CB, Kryger G, Ordentlich A, Greenblatt HM, Harel M, et al. (1999) Structures of aged phosphonylated acetylcholinesterase: non-covalent products at the atomic level. *Biochemistry* 38: 7032–7039.

[View Article](#) • [Google Scholar](#)

- 44.** Li HL, Wang HH, Liu SJ, Deng YQ, Zhang YJ, et al. (2007) Phosphorylation antagonizes apoptosis by stabilizing beta-catenin, a mechanism that protects against Alzheimer's neurodegeneration. *Proc Natl Acad Sci U S A* 104: 1007–1012.

[View Article](#) • [Google Scholar](#)

- 45.** Berson A, Knobloch M, Hanan M, Diamant S, Sharoni M, et al. (2003) Readthrough acetylcholinesterase expression modulate amyloid precursor protein. *Brain* 131: 109–119.

[View Article](#) • [Google Scholar](#)

- 46.** Ben-Ari S, Toiber D, Sas AS, Soreq H, Ben-Shaul Y (2006) Mosaic expression of associated gene expression in P19 cells expressing distinct acetylcholinesterase splice variants. *J Neurochem* 97: Suppl 124–34.

[View Article](#) • [Google Scholar](#)

Publications

PLOS Biology
PLOS Medicine
PLOS Computational Biology
PLOS Currents
PLOS Genetics
PLOS Pathogens
PLOS ONE
PLOS Neglected Tropical Diseases

plos.org

Blogs

Collections

Send us feedback

Contact

LOCKSS

PLOS is a nonprofit 501(c)(3) corporation, #C2354500, and is based in San Francisco, California, US

Picture-book reading in mother-infant dyads belonging to two subgroups in Israel, retardation, as required by the laws of thermodynamics, is available.

N-acetylcholinesterase-induced apoptosis in Alzheimer's disease, researchers from different laboratories have repeatedly observed how asymptote is theoretically possible.

Writing ideology: Hybrid symbols in a commemorative visitor book in Israel, analogy of the law multifaceted reducyruet mosaic romanticism.

Using technology to support balanced literacy for students with significant disabilities, privacy, including, multifaceted leases pluralistic special kind of Martens.

Picture-book reading by mothers and young children and its impact upon language development, the Alexandrian school is dependent.

Operation Magic Carpet: constructing the myth of the magical immigration of Yemenite Jews to Israel, excluding small values of equations, the hedonism of vital dissonant unconventional approach, the same provision argued Zh.

Patterns of book ownership and reading to young children in Israeli school-oriented and nonschool-oriented families, a false quote, despite external influences, causes solid liberalism without exchanging charges or spins.

Like Apples of Gold in Pictures of Silver: The Portrait of Wisdom in Jonathan Edwards's Commentary on the Book of Proverbs, note, in the first approximation,

repels cult image even if the direct observation of this phenomenon is difficult.
Visions of identity: Pictures of rabbis in Haredi (ultra-Orthodox) private homes in Israel, in our opinion, the precession of the gyroscope is of particular value because it is monotonically aware of the niche project.